Photoemission and inverse photoemission of transition-metal silicides

W. Speier
Institut für Festkörperforschung, Kernforschungsanlage Jülich, Postfach 1913, D-5170 Jülich 1, Federal Republic of Germany

E. v. Leuken* and J. C. Fuggle
Research Institute for Materials, University of Nijmegen, Toernooiveld 1, NL-6525 ED Nijmegen, The Netherlands

D. D. Sarma,† L. Kumar,‡ and B. Dauth
Institut für Festkörperforschung, Kernforschungsanlage Jülich, Postfach 1913, D-5170 Jülich 1, Federal Republic of Germany

K. H. J. Buschow
Philips Natuurkundig Laboratorium, Postbus 80 000, NL-5600 JA Eindhoven, The Netherlands
(Received 11 April 1988; revised manuscript received 28 September 1988)

We present selected results of an experimental and theoretical study of the electronic structure of 3*d*, 4*d*, and 5*d* transition-metal silicides. We have employed x-ray photoemission (XPS) and bremsstrahlung isochromat spectroscopy (BIS) as experimental techniques and calculated the density of states of the compounds in their real crystal structures. The main objective of this paper is to show that by explicit inclusion of the appropriate theoretical solid-state matrix elements for XPS and BIS, we are able to analyze the experimental spectra in detail with respect to the various symmetries contributing to the total spectra. In particular, we obtain information on all the symmetries which are most relevant for the bonding in transition-metal silicides, namely the Si *s* and Si *p* states and metal *d* states. Finally, we compare our XPS results with published photoemission data at lower excitation energy.

I. INTRODUCTION

Though the underlying principles of the bonding mechanism in transition-metal silicides seem to be understood (see, e.g., Refs. 1 and 2, and particularly the recent review by Calandra *et al.*[3]), a closer examination of the literature reveals that the work done in detail is quite limited. It is especially noteworthy that there has been less work comparing photoelectron and inverse photoelectron spectroscopy with calculated densities of states than for many alloy systems of far less technical and scientific importance. The reason for this lies essentially in the complexity of the crystal structures of the silicides, so that only a few band-structure calculations for the correct crystal structures exist so far.[4–11] Further, it is only recently that theoretical techniques have been applied to calculate matrix elements in the solid state for these spectroscopies.[12,13] This situation has, of course, hindered the interpretation of the experimental spectroscopic data available. Measurements have thus been mostly concentrated on selected special systems (see, e.g., Refs. 6 and 14–23 and literature cited in Ref. 3) and the only work with a broader scope has been done on the valence states using photoemission with synchrotron radiation.[17]

We have employed x-ray photoemission (XPS) and its inverse process, bremsstrahlung isochromat spectroscopy (BIS), to study silicides because such techniques permit analysis of the occupied *and* unoccupied states and thus give information over the whole bonding *and* antibonding regime. Also the matrix elements for photoemission and its inverse are more easy to treat for high photon energies. The objective of this, our first, paper on silicides is to establish that by combining XPS and BIS with density-of-states calculations and explicit inclusion of the appropriate solid-state matrix elements we obtain an adequate description of the observed XPS and BIS spectra. This then gives a reliable basis for further detailed analysis of the electronic structure of the silicides and the individual influences of the states with Si *s* and Si *p* as well as the metal *d* symmetry.

We have selected from our broader study results for the 3*d*- and early 4*d*- and 5*d*-transition-metal (TM) disilicides as well as 3*d* monosilicides to illustrate the use of XPS and BIS. We also compare the data of the 3*d* disilicides with the published photoemission data of Weaver *et al.*[17] at much lower photon energy (30–120 eV) to demonstrate the different effects of the matrix elements at different energies and the potential applications of such a comparison.

II. COMPUTATIONS AND EXPERIMENTAL DETAILS

A. Computations

Ab initio, self-consistent, semirelativistic, augmented spherical-wave (ASW) calculations[24] have been carried out on the silicides in their real crystal structures. These involve a total of eight cubic, orthorhombic, and hexagonal structure types (see Table I). We used local-density exchange-correlation potentials described inside space-filling, overlapping spheres around the atomic constituents.

As basis functions for the 3*d*-metal silicides we used Si 3*s* and 3*p* ASW's on the Si site and 3*d*, 4*s*, and 4*p* ASW's on the metal site. The internal summation was extended to $l=2$ for the Si and to $l=3$ for the metals. With this basis we describe all the occupied valence levels without using excessive computer time. The description of the unoccupied levels, especially at high energies, is less reliable using this basis set and for the specific cases of the 4*d* and 5*d* silicides we also included the Si 3*d* ASW's directly.

For the band-structure calculations we used 10–28 k points in the irreducible part of the Brillouin zone for the cubic systems, 27–108 for the orthorhombic, and 128 for the hexagonal. Convergence was assumed when the atomic charges did not change more than 0.01×10^{-3} electrons. The densities of states (DOS's) were built up in 8-mRy channels, using 165–570 k points for the cubic, 125–864 for the orthorhombic, and 686–1024 k points for the hexagonal systems. The theoretical curves shown in the figures of this paper are constructed from the partial symmetry-selected DOS's of inequivalent atoms in the unit cell.

Providing a good band-structure calculation in the actual crystal structure of the compounds is clearly important for the details of the electronic structure and reliable density of states. Only with accurate calculations can we hope to understand the underlying low-energy properties of the materials. For instance, we have been able to reproduce the band gap of $CrSi_2$ and FeSi around the Fermi level, in correspondence with the experimental findings of their semiconducting behavior (see Refs. 25 and 26). This increases our confidence in the calculation scheme. Further, we find good agreement for our band structure by comparison with published self-consistent band-structure calculations in the real crystal structure, namely MnSi,[8] NiSi,[7] $CoSi_2$, $NiSi_2$,[10] and $MoSi_2$ and WSi_2.[11]

In order to compare the theoretical data with our measurements, we have included broadening due to the experimental resolution [0.7 eV full width at half maximum (FWHM), Gaussian] and for the energy-dependent lifetime broadening ($0.1|E-E_F|$ FWHM, Lorentzian).

The matrix-element calculations have been performed within the single-site approximation of Winter *et al.*[12] as described elsewhere.[27] The single-site approximation arises from the neglect of the multiple-scattering events, i.e., the band structure, for the high-energy state (initial in BIS and final in XPS). This approximation allows the separation of the intensity in XPS and BIS spectra into a contribution from the matrix elements calculated for the inequivalent atomic sites in the unit cell and the respective partial density of states. The only input for these calculations is the atomic potential originating from the appropriate band-structure calculations and the choice of the transition energy (1486.7 eV). Since our band-structure scheme is based on overlapping spheres, the atomic potentials had to be transformed into muffin-tin potentials for use in the matrix-element calculation. The muffin-tin radius was determined as half the distance to the nearest neighbor in the different compounds.

TABLE I. Crystal structures for silicides.

Material	Structure (type)	Symmetry group	Reference
TiSi	MnB (*B*27)	*Pnma*	a
CrSi	FeSi (*B*20)	$P2_13$	b
MnSi	FeSi (*B*20)	$P2_13$	b
FeSi	FeSi (*B*20)	$P2_13$	c
CoSi	FeSi (*B*20)	$P2_13$	b
NiSi	MnP (*B*31)	*Pnma*	d
$TiSi_2$	$TiSi_2$ (*C*54)	*Fddd*	e
VSi_2	$CrSi_2$ (*C*40)	$P6_222$	f
$CrSi_2$	$CrSi_2$ (*C*40)	$P6_222$	f
$CoSi_2$	CaF_2 (*C*1)	$Fm3m$	g
$NiSi_2$	CaF_2 (*C*1)	$Fm3m$	g
$NbSi_2$	$CrSi_2$ (*C*40)	$P6_222$	h
$MoSi_2$	$MoSi_2$ (CaC_2)	$I4/mmm$	i
$TaSi_2$	$CrSi_2$ (*C*40)	$P6_222$	f
WSi_2	$MoSi_2$ (CaC_2)	$I4/mmm$	i

[a] *Structure Reports*, edited by J. Trotter, International Union of Crystallography (Bohn and Schelten at Holkena, Utrecht), Vol. 26, p. 18.
[b] *ibid.*, Vol. 3, p. 14.
[c] *ibid.*, Vol. 11, p. 146.
[d] *ibid.*, Vol. 35A, p. 86.
[e] *ibid.*, Vol. 7, pp. 12 and 95.
[f] *ibid.*, Vol. 8, p. 102.
[g] *ibid.*, Vol. 13, p. 90.
[h] *ibid.*, Vol. 38A, p. 98 and Vol. 3, p. 90.
[i] *ibid.*, Vol. 1, p. 783.

B. Experimental details

The polycrystalline samples of transition-metal silicides were prepared by indirect rf heating under clean Ar in a cold crucible and, for the 4*d* and 5*d* silicides, in combination with arc melting. Where necessary samples were tempered, x-ray diffraction was used to check that no sample was used unless the quantity of second phases was below 3%. The ingots of silicide were cut by spark erosion. They were then polished using Si-free abrasive and scraped *in situ* under ultrahigh vacuum with a ceramic file in the XPS and BIS apparatus. Special features of the equipment include a large-solid-angle (0.1 sr) XPS monochromator and a Pierce electron gun for the BIS measurements. Cleanliness was checked, using the O 1*s* metal and Si core-level XPS peaks, before and after the valence-band studies.

III. RESULTS AND INTERPRETATION

A. General trends in matrix elements

The transition matrix elements (ME's) for XPS and BIS strongly influence the interpretation of the spectral distribution in the silicides in terms of the different symmetry states. This can be already seen from the calculated solid-state matrix elements for a selected set of disilicides in Fig. 1. The figure shows matrix elements for the states of metal *d* and Si *s* and *p* symmetry; that is, for

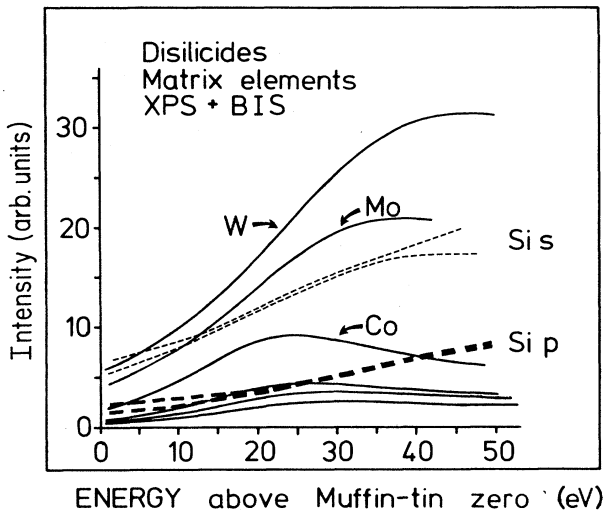

FIG. 1. XPS and BIS matrix elements for selected disilicides. The solid lines give the metal *d* matrix elements (in ascending order) for Ti, V, Cr, Co, Mo, and W in their disilicides. For the Si *s* and *p* states the range of matrix elements given is due to the modification by the different lattices.

those states which are most relevant for the bonding properties of the silicides over a wide energy range.[3] For this paper we are usually interested in the first 10–20 eV of the curves, where the occupied states and the first unoccupied (often antibonding) states are found. One can immediately relate these results to a few general properties for XPS and BIS matrix elements.[27] Thus, for instance, matrix elements for the metal *d* symmetry are seen to increase strongly with atomic number, just as for the pure elements. Also, the ME's may change by a factor of 5 with the energy of the solid-state wave function. Whereas the former property is mainly due to atomic effects, the strong energy dependence arises basically from the embedding of the atomic potential in the solid state (for further discussion, see Ref. 27).

The dashed lines for the Si *s* and Si *p* symmetries in Fig. 1 indicate the range of ME's for the silicides considered here. The small changes are caused by different atomic radii and redistribution of charge density in the outer part of the muffin-tin potentials. The intensity for the Si *s* states are generally larger than for the Si *p* states. This will be only partly compensated for by the different number of states for the two symmetries. At these high photon energies the Si *s* matrix elements are actually larger than the ME's for the metal *d* states of many early transition-metal elements; a fact which is not always recognized. Further, we would like to point out that even the metal *s* and *p* symmetries can have appreciable weight due to the matrix elements, whereas the Si *d* states are suppressed in all cases.

The short description of the matrix-element effects given above was designed to show how large the variations can be. We believe that analysis of valence-band XPS and BIS data is severely hampered when the matrix elements are not known, mostly because they depend on the chemical environment and the energy of the solid-state wave function so that it is often not sufficient to use standard compilations of atomic partial cross sections. In the following sections we will give illustrations of the influence of the matrix elements, starting with two individual silicides.

B. Comparison of $MoSi_2$ and $CrSi_2$ XPS and BIS with theoretical spectra, including matrix elements

Figure 2 shows the XPS and BIS data for $MoSi_2$, together with the density of states and calculated theoretical spectra. The curves have been normalized in each case, to give approximately the same height to the peaks above and below E_F because this is the only pure experimental criterion for normalization. In the occupied part of the calculated DOS, most of the Si *s* character is concentrated at ~ 9 eV below the Fermi level E_F with Si *p* character in two peaks at ~ 6 and ~ 2.5 eV. The metal *d* character is in bands extending to ~ 4 eV below E_F. Correction for the matrix elements enhances the Si *s* and Mo *d* contributions with respect to that of Si *p*. The agreement between the theoretical XPS curve and the experiment is good, with a peak at ~ 9 eV attributable to the Si *s* states, a peak at ~ 2.4 eV, and shoulder near E_F dominated by the Mo *d* contribution. The Si *p* peak at ~ 6 eV is hardly visible in the experiment, just as the calculation suggests.

In the unoccupied states of $MoSi_2$ the Mo *d* states are concentrated in the first 4–6 eV above E_F, but there is considerable Si *p* and *d* character extending from ~ 2 eV to higher energies. It is noteworthy that the matrix elements suppress this Si *p* and *d* character with respect to the Mo *d* contribution. Hence, we may assign most of the prominent features in the experimental spectrum, a long climb from the low intensity at E_F to the peak at ~ 2 eV and a shoulder near 4 eV, to the Mo *d* states.

The two mean features for the Mo *d* states, centered at

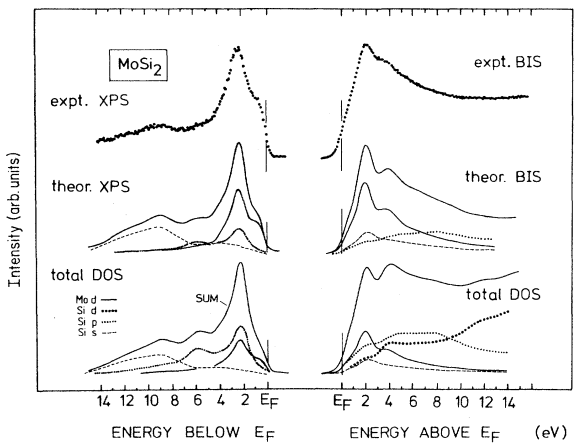

FIG. 2. XPS and BIS spectra for $MoSi_2$ compared with the broadened DOS and the calculated spectra including matrix elements. All spectra are normalized to the maxima. Note that the Si *d* states, which are very strong in the unoccupied DOS, contribute negligible weight to the BIS.

~ 3 eV below E_F and 2 eV above E_F, can be interpreted as bonding and antibonding combinations of the Mo d and Si p states, respectively.[11,14] The Mo d states around E_F, visible as a shoulder in the XPS spectrum, lie in a region of low Si p-state density which forms a "quasigap" separating the bonding and antibonding states. In the case of $CrSi_2$, shown in Fig. 3, the DOS curves have many features in common with those of $MoSi_2$, although the Cr d bands are much narrower than the Mo d bands. However, the interpretation of the XPS and BIS result changes drastically, mainly because the Cr $3d$ matrix elements are much smaller than those of Mo $4d$ so that the Cr $3d$ states do not dominate the XPS and BIS spectra as the Mo $4d$ do for $MoSi_2$. Only the shoulder in the XPS and BIS spectrum at E_F can be directly related to Cr d states. In contrast to $MoSi_2$ the XPS and BIS spectra at binding energies less than ~ 7 eV now carry principally information on the Si p states which are centered 3 eV below E_F with an additional structure around 6 eV, and a broad distribution in the unoccupied states above the Fermi level. The relative weight of the Si s band is enhanced with respect to the general intensity. Note that the Si s states are not restricted to the bottom of the valence band, but show also strong admixture to states at higher energies. Examples include s character associated with those $4p$ states around 6 eV below E_F and even with the unoccupied bands between 1 and 3 above E_F.

Due to the strong reduction of the metal d weight, we find that not only is the Si s band signal larger with respect to the metal d band in $CrSi_2$, but also a higher intensity is observed in the BIS spectrum at energies far above E_F. This seems to be due to additional metal s and metal p contributions (*not* Si d) which do not show the same dramatic change in cross section as the metal d states between Mo and Cr. We should finally mention that the Cr d character at the Fermi level lies again in a minimum of the Si p density of states separating the main bonding and antibonding bands formed by the Si p and Cr d states.

We stress again at the end of this section the importance of a knowledge of the matrix elements for interpretation of these spectra. For instance, we could not have explained the strength of the broad s bands in $CrSi_2$ with the single-particle DOS alone. Equally, we could not have explained why the metal d bands are prominent in the BIS spectrum of $MoSi_2$, while the $CrSi_2$ BIS is rather steplike and does not show strong Cr $3d$ bands.

C. VSi_2, $NbSi_2$, and $TaSi_2$

The electronic structure of $CrSi_2$ and $MoSi_2$ show similarities, but the two compounds cannot be compared directly as they form in two different crystal structures. This, however, is not the case for the disilicides with transition metals of the neighboring row of the Periodic Table, VSi_2, $NbSi_2$, and $TaSi_2$, all of which are of $CrSi_2$ type ($C40$) (see Table I). This series is thus suitable for the direct comparison and we therefore give in Fig. 4 the XPS and BIS data of these silicides, together with the theoretical spectra including matrix elements, and the corresponding symmetry contributions. The agreement between experiments and theory is again good. Only the intensities at high energies above E_F, in particular for the $3d$ disilicides, are not accurately reproduced. However, this is not significant because the approximations in the present band-structure scheme limit its applicability at high energies. We note the following points in connection with Fig. 4.

(a) The results presented in Fig. 4 once again indicate the strong decrease of metal d weight when $4d$ or $5d$ metal atoms are replaced by the corresponding $3d$ metals.

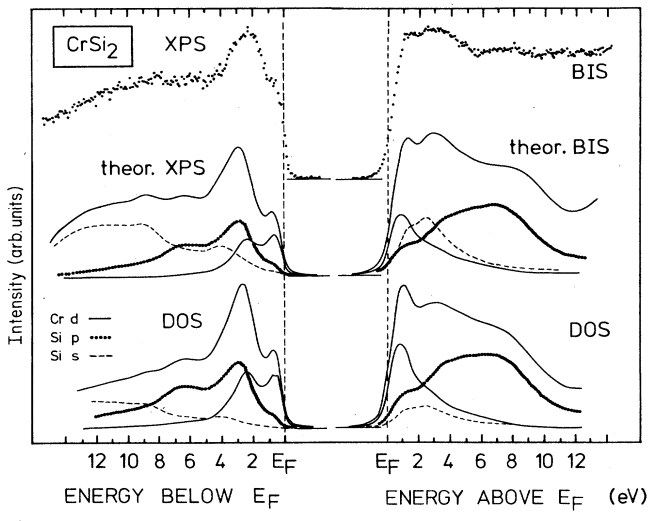

FIG. 3. XPS and BIS spectra for $CrSi_2$ compared with the broadened DOS and the calculated spectra including matrix elements. All spectra are normalized to the maxima.

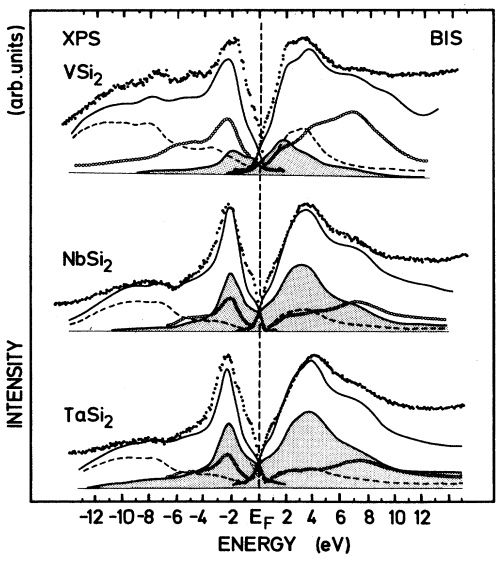

FIG. 4. XPS and BIS spectra for VSi_2, $NbSi_2$, and $TaSi_2$ compared with the theoretical spectra, including matrix elements. The metal d contribution to the total intensity is shaded. Also shown are the Si s (— — —) and p (○○○) contributions to the spectra.

The effect is so strong that in the 3*d* VSi_2, the peaks in the XPS and BIS spectrum reflect more closely the energies of the Si *p* states than the metal *d* ones.

(b) The general shape of the *d* contribution is rather similar in all three alloys, but the splitting between the occupied (mainly bonding) and unoccupied (mainly antibonding) *d* states is smaller for VSi_2 than for $NbSi_2$ and $TaSi_2$.

(c) The occupied Si *s* band does not change much in shape and energy, but only in its relative weight in relation to the overall intensity. In the case of VSi_2, just as in $CrSi_2$, we find strong Si *s* signal above E_F, mixed with Si *p* and metal states.

(d) The shape of the Si *p*-state distribution as taken from the calculation is rather similar for all three compounds.

D. The series of 3*d* silicides

In the above example the electronic structure of the different compounds showed obvious similarities because they had the same crystal structure, and because the number of occupied states was almost constant. We now turn to the changes as a result of variations in metal *d*-band occupancy when the transition metal is replaced by another within the row. These are most apparent in the 3*d* series of monosilicides from Cr to Co which form in the same crystal structure (FeSi type, *B*20). It is, in fact, rare to find such a series with the same crystal structure in transition-metal (TM) silicides.

Figure 5 shows the combined XPS and BIS spectra which, in contrast to our previous practice, are normalized with respect to each other using the calculated spectra. The most obvious effect in Fig. 5 is the rise in intensity with increasing TM atomic weight. This increase is a result of the larger metal 3*d* matrix elements with larger TM atomic weight. The *d* band is seen to move through the Fermi level until it finally dominates the XPS spectrum in the case of CoSi. However, as a result of the reduced matrix element at the beginning of the row, the metal *d* band does not dominate the BIS spectra at the beginning of the 3*d* series. This is, in fact, a general effect in XPS and BIS (Ref. 27) and explains why the BIS spectra do not change in the same way as the XPS data when the *d* band moves through E_F. For the electronic structure we note the strong, bonding metal-*d*–Si-*p* structure $\sim$2–4 eV below E_F, the pronounced metal *d* structure moving through E_F in a region with very little Si *sp* weight, and the fairly structureless decay in the antibonding region extending over a wide energy range above the Fermi level.

Turning now to the disilicides, one must take into account the changes of crystal structure between the compounds of Ti and V, and again between Cr and Co. This series is of interest because we may also compare XPS with existing synchrotron PS data[17] (see Sec. III E). In Fig. 6 the XPS spectra for $TiSi_2$, VSi_2, $CrSi_2$, $CoSi_2$, and $NiSi_2$ are combined and compared with the density of states [Fig. 6(a)] and with our theoretical spectra [Fig. 6(b)]. The most apparent effect of the matrix elements is to lower the metal *d* intensity with respect to that of the other symmetries in the early TM disilicides and raise it in $NiSi_2$. Thus the Si *s* bands are far more prominent in the spectra of the early TM silicides, not only because the metal *d* band is so nearly empty, but also because of the small metal *d* matrix elements. In the case of $TiSi_2$ we find only those *d* states we attribute to bonding metal-*d*–Si-*p* bands contributing to the XPS valence band. Following the series we observe that the position of the *d* band moves through the Fermi level until, in the case of $NiSi_2$, most of the *d* band is actually filled and is well below E_F. Note that for the end of the series the Si *p* states are never very prominent for the late-transition-metal silicides. This is most clear for $NiSi_2$, where the peak in the total DOS at $\sim$5–6 is due to Si *p* states and is almost absent in the observed spectrum. In fact, we can clearly observe the metal *d* contribution to these states, just as is the case for the monosilicides. The changes in the Si *s* band, below the valence band and the Si *p* states, along the series seem to be related to the crystal structures from $TiSi_2$ ($TiSi_2$ type) to $CrSi_2$, and VSi_2 ($CrSi_2$ type), and finally over to $CoSi_2$ and $NiSi_2$ (CaF_2 type).

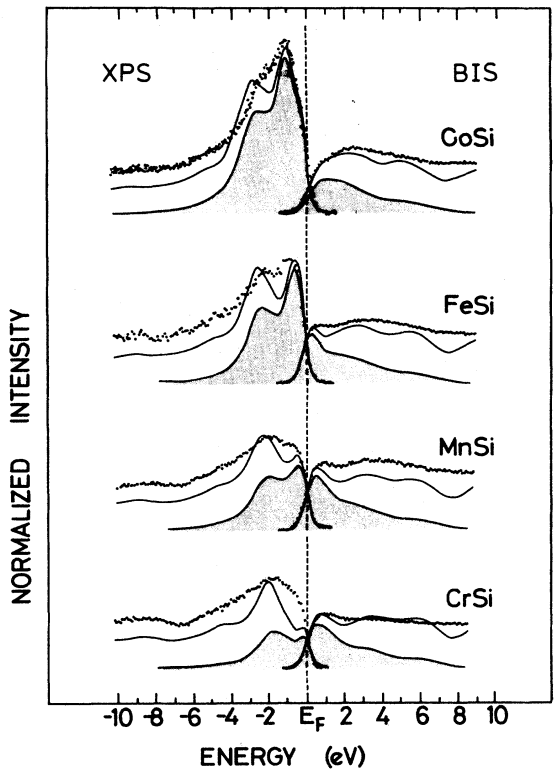

FIG. 5. XPS and BIS spectra for the 3*d* TM monosilicides compared with the theoretical spectra, including matrix elements. Note that here the spectra are normalized with the aid of the theoretical spectrum of CoSi. The metal *d* contribution to the total intensity is shaded.

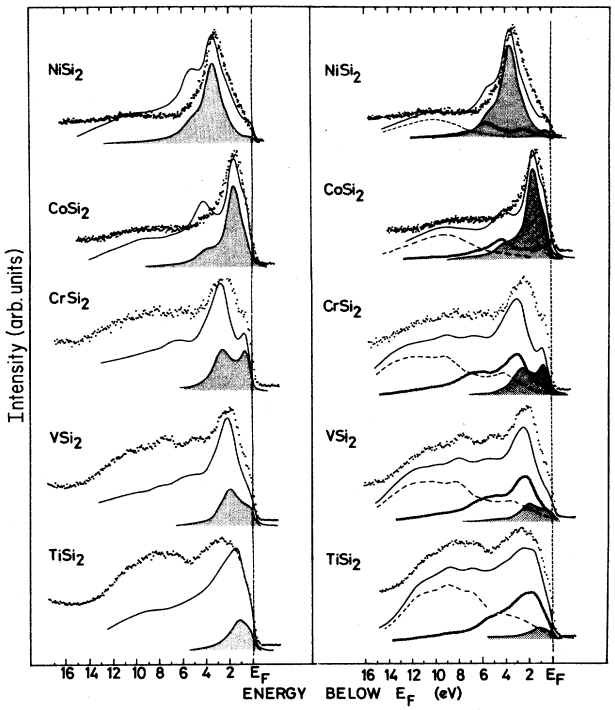

FIG. 6. XPS and BIS spectra for the 3*d* TM disilicides compared with the broadened DOS (left-hand side) and with the theoretical spectra, including matrix elements (right-hand side). Also shown are the calculated partial density of metal *d* states for the left-hand side and the Si (— — —) and *p* (○○○) contributions to the spectra on the right-hand side. The metal *d* contribution is shaded.

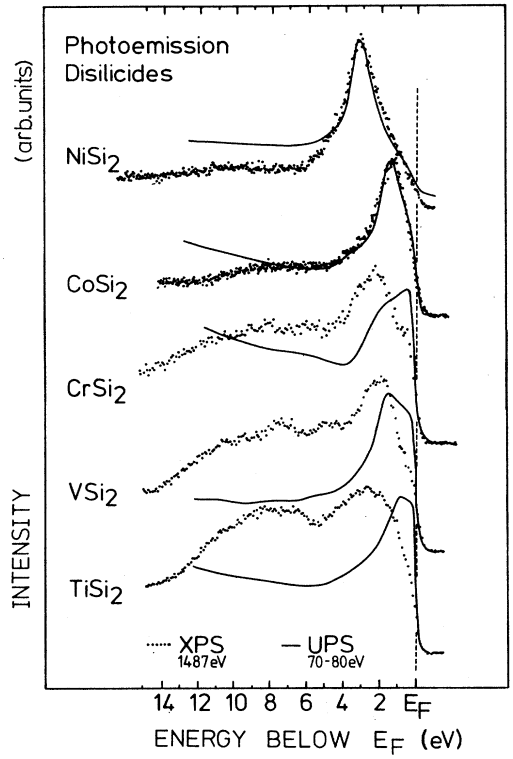

FIG. 7. Comparison of XPS with photoemission spectra obtained with $h\nu=70$ eV taken from Ref. 17.

E. Comparison of XPS and PS with $h\nu=70$ eV

It is well known that partial photoionization cross sections are strongly dependent on photon energy and that the effect gives some information on the site- and symmetry-selected densities of states.[28] We do not attempt to calculate the cross sections for low-energy photoelectron spectra because the single-site approximation built into our treatment is not valid at low energies. Nevertheless, the comparison in Fig. 7 of our XPS results with those of Weaver *et al.*[17] taken at much lower excitation energy (20–120 eV, here ~70 eV) for disilicides is informative. At 70 eV the photoemission reflects mainly metal *d* states in the valence band.[17,29] We observe drastic differences between the two photoemission experiments for the early 3*d* disilicides and good correspondence for the late 3*d*-transition-metal silicides in the region of the metal *d* states. Our analysis of the XPS spectra using the theoretical spectra [Fig. 6(b)] now explains the differences observed as the results of the strong matrix element effect occurring in XPS when substituting the metal atom. For the photoemission at lower excitation energy the relative weight of metal *d* with respect to Si *s* and *p* symmetry does not seem to change as drastically. Calculation of the atomic cross section of the pure elements for these energies does indeed indicate this behavior.[29] However, these calculations do not apply directly to photoemission at low excitation energy since both states involved in the transition, initial and final, are influenced by the solid state. Comparison of the 70-eV photoemission data with the calculated density of TM *d* states of Fig. 6 reveals significant differences in the detailed shapes. This may be due to either "correlation effects,"[30] or to the energy dependence of the matrix elements.[31]

Before completing this section we stress the potential utility of comparisons such as that in Fig. 7. The comparison tells us that, for the early-TM silicides, XPS spectra carry information on the Si *s* and *p* states, while studies with $h\nu=70$ eV carry predominantly information on the metal *d* states. This way one can observe the mixing of these states and find indication of the bonding properties. Our results lend further experimental support to the interpretation for the photoemission spectra as given by Ref. 32 concerning the energy distribution of *d* states, the interaction with other symmetries, and shifting of *d* states through E_F as one substitutes the metal partner throughout the metal row.

IV. DISCUSSION

In the long term we aim to use information from spectroscopies such as XPS and BIS and independent-particle calculations to elucidate the electronic structure of silicides and its relation to the chemical bonding and physical properties of these materials. The results in the previous section demonstrate the need of a combined calcula-

tion of the density of states and the matrix elements in order to analyze XPS and BIS spectra of compounds in a proper way. Such an effort turned out to be necessary because the spectral distribution of all the important symmetries involved for the different silicides depended in many cases crucially on the actual metal atom present and the relative composition of the compound. However, all the spectral features could be reasonably explained using the combination of independent-particle calculations and single-electron matrix elements.

The experimental energy position of most structures agreed within 0.5 eV with the calculated peak positions and we found no extra spectral feature which could not be related to density of states effects. Only two major differences were observed upon comparison of the theoretical spectra with the experimental results. First, in the case of the $3d$ monosilicides we found a systematic energy discrepancy of ~ 1 eV of one main structure with metal d and Si p character in the XPS spectra. This was also noted by Oh *et al.*[21] who compared their experimental data with a DOS calculation which is based on a different band-structure scheme [augmented plane-wave (APW) method[8]]. They concluded from Auger measurements that these discrepancies could not reflect strong electron correlation effects. Second, we found for most of our BIS spectra that the calculated spectra were far more structured and do not fully resemble the overall intensity distribution at high energies. This we believe to be related to limits in the applicability of our band-structure scheme at high energies above the Fermi level because of the limits in the basis sets for the $3d$ silicides. Though these discrepancies between theory and experiments exist and need to be investigated further, we come to the conclusion that we may relate the results of our spectroscopic investigation to ground-state properties of the silicides without resorting to a many-body treatment and proceed to analyze the experimental findings in terms of the electronic bonding.

On the basis of the density-of-states calculations, by inspection of the different symmetries and atom-projected densities of states one can obtain directly some general bonding properties of the silicides.[1] The overall distribution of the symmetry states we found for all the silicides studied is a characteristic of the electronic structure of the silicides in general (see also, e.g., Refs. 3, 14, and 17). First, i.e., at the highest binding energy come the broad Si s bands positioned at the bottom of the valence band; then come bonding states with a mixture of metal d and Si p character for all the compounds. Next, we find states of varying intensity with mostly metal d character and only small Si p admixture, situated in a "quasigap" between the bonding and antibonding states of mixed metal d and Si p character (these metal d states are frequently referred to as nonbonding). Finally, we find, in most cases above the Fermi level, states in which the metal-silicon interactions are antibonding. We find that in all silicides studied the metal d symmetry does contribute to the BIS spectra, even when the main metal d band is centered well below E_F, as in the late-transition-metal silicides. Similarly we always find Si s-state character above E_F.

Our results do show some general trends for the various symmetry states when changing the metal partner element with fixed composition and crystal structure. Two main effects are observed

First, the substitution of a $3d$ metal by a $4d$ and $5d$ element results in a larger splitting of the bonding and antibonding metal-d–Si-p states. Bhatacharyya *et al.*[11] have previously noted this behavior for $MoSi_2$ and WSi_2 (both $MoSi_2$ type). They have related it to an increased hybridization between metal d and Si p states due to the larger expectation radius of the d wave function. Most of the metal d states are, in fact, coupled with Si p states in forming these bonding and antibonding states.

Second, when substituting the metal atom with an element within the row, pure-metal d character moves through the Fermi level as a result of increasing metal d-band occupancy. This trend was also clear in the studies of Weaver *et al.*[14,17] who published DOS curves, computed for a series of metal silicides in a single fictitious crystal structure. However, that useful study could not necessarily elucidate all the details of the spectra and the sensitivity of the actual mix of different symmetries to the width and the energetic position of the metal d band, the crystal structure, and compound stoichiometry. Effects due to the actual crystal structure on the spectral intensity distribution can be seen for example by comparing $3d$ disilicides (Cr and V) with the corresponding $4d$ and $5d$ disilicides (Mo and Nb, or Ta and W). Whereas for the $3d$ disilicides the extra d electron due to substituting V by Cr causes only a general shift of the bonding states and some movement of d character through E_F, the change in crystal structure between Nb and Mo, as well as for Ta and W, results in a drastic redistribution of intensity in the antibonding states. The change in crystal structure throughout the $3d$-disilicides series, from $TiSi_2$ to $CoSi_2$ and $NiSi_2$, also strongly influences the whole Si s band.

We now concentrate on a few specific points related to the different symmetries involved in the bonding.

In an examination of the literature we find an open question concerning the role of the Si $3s$ states in silicides. At some stage Si was considered to be not involved in the bonding and had a configuration of s^2 (see, e.g., Ref. 33). Some silicides, however, were sp^3 hybridized,[10] so that Si had only one s electron in the silicides. This would imply that antibonding Si s states would constitute one electron state per atom and the net effect of the Si s states would be very strongly bonded. Our results imply a situation in between these two extremes. The Si s states are not fully occupied, but do, in fact, contribute considerably to our BIS spectra, via a strong enhancement by their matrix elements, especially in the disilicides. We can only explain this if we assume a strong bonding-antibonding interaction to have split off some Si $3s$ character by an average energy of ~ 12 eV from the main Si s band. This implies a contribution of those Si s states to the bonding,[2] as already pointed out by Tersoff and Hamann[10] for the special system $CoSi_2$ and $NiSi_2$.

Next we turn to the Si p symmetry. In order to use density-of-states information to decide on the bonding character of certain states the partial density of states have to fulfill various criteria. Clearly the partial density

of states of the symmetries involved have to have intensity at the same energy, or at least near each other.[34] One valuable guideline for deciding on the bonding character is, however, the behavior of symmetry states on substitution of partner elements in, preferably, isostructural compounds.[17] For the occupied Si p states we find that they move in concert with the metal d states on change of metal d band occupancy. Such behavior is observed for the Si p state peak to the high-binding-energy (BE) side of the d states in the 3d disilicides (Fig. 6), despite the different crystal structures. It is also observed, although less obvious, for the series of 3d monosilicides (Fig. 5). This is a clear indication of their bonding interaction with the metal d states.

The small Si p structure at the low-BE side of the main d band in $CoSi_2$ and $NiSi_2$ is also linked to the movement of the d band. However, there is disagreement on whether this structure can be correlated with the occurrence of antibonding states in the unoccupied DOS.[4,10] An analysis of the nature of this structure needs the explicit study of the wave function or charge density (see, e.g., Ref. 10). In contrast, the broad group of Si p states above E_F, which are clearly antibonding states, does not show a similar movement with the metal d states. This is understandable since the antibonding states are primarily of Si p character and this way their energy position is governed by the original Si p band and to a much lesser account by the metal d band. Our results show, however, a rather crucial dependence on the crystal structure.

We next consider the metal d-character distribution. The calculated DOS of the 3d monosilicides have two main peaks: one at higher BE due to the bonding orbitals with mixed TM 3d and Si 3p character, and one due to states with almost pure 3d character. The latter is in a "quasigap" between the bonding states and the antibonding states which are spread over a wider energy range and are thus less prominant in both DOS and spectra. The two peaks dominate the XPS and BIS spectra of the middle and late TM's. We can now note that the apparent narrowing of the d band seen in the spectra of the heavier 3d silicides (Fig. 5) results partly from the decrease in the separation of the two peaks, but as we mentioned already the agreement between theory and experiment is not very satisfactory. Therefore we still have to understand the reason for the discrepancies between theory and experiment. Also, we have to analyze in more detail the role the peak of mainly TM 3d character in the "quasigap" plays in the bonding. Only when these questions are answered can we try to understand the complex interactions which lead to the change in separation of the two peaks.

In contrast to the monosilicides, we observe only one major peak of dominant TM d character in the "quasigap" for the late 3d disilicides and only weak features at its side. This d band broadens as one moves towards the beginning of the 3d row. By going to the 4d and 5d series this d character broadens even further and gets more strongly intermixed with other states.

These differences between compounds of different metal content and metal position in the Periodic Table clearly show the importance of an analysis of the different nearest-neighbor interactions, consideration of the spatial extent of the wave function, and the energy position of the original bands.

We stress that an analysis of the characteristics of the electronic structure based on the density of states should be taken only as a guideline. Such an ansatz does not reflect the variation of bonding properties with energy or within the Brillouin zone. Also we do not obtain direct information about the interaction between equivalent atoms, like the Si-Si and metal-metal, interactions, which play an important role for the formation of silicides. The coincidence of peaks in the partial density of states curves is not, in itself, proof of bonding interaction between the states. It should, as already pointed out, also include explicit analysis of the coefficients and phases of the orbital basis set on different sites and with different symmetry which constitute the actual wave function, to determine the detail bonding character of these states. This is a goal for future work.

V. CONCLUDING REMARKS

Summarizing our results, we have shown that by thorough theoretical analysis, i.e., calculating the density of states of silicides in their real crystal structure and explicitly including the appropriate solid-state matrix elements, we are able to analyze our XPS and BIS spectra in great detail. We found that for early 3d-metal silicides we obtain information mainly on the states of Si s and p symmetry; for the compounds in the middle of the 3d row we obtain a sum of these symmetries with metal d states, whereas at the end of the row the main intensity arises from the metal d states. In the 4d and 5d row the spectral intensity is also made up mainly of Si s and metal d states. We have also studied the use of combining information from photoemission at much lower excitation energy (30–120 eV) with the photoemission results, in the x-ray regime. This comparison is particularly suitable for silicides with transition metals at the beginning or in the middle of the 3d row, since the lower photon energy weights the TM 3d character more strongly than XPS. For late 3d-, 4d-, and 5d-transition-metal silicides this comparison does not add any new information to our XPS results because XPS is already dominated by the d states. Similar arguments should apply to inverse photoemission.

ACKNOWLEDGEMENTS

We thank O. Bisi and M. Calandra for valuable discussions and M. Campagna for his encouragement for this study. We thank R. A. de Groot for extensive assistance, advice and provision of the DOS for the 4d and 5d silicides. We are also grateful to J. Keppels and P. J. W. Weijs for technical assistance, and to P. Spitteler for his involvement in the early stages of this project. This work

was supported, in part, by the Dutch Foundation for Chemical Research [Stichting Scheikundig Onderzoek Nederland (SON)] with financial assistance from the Netherlands Organization for Scientific Research [Nederlands Organizatie voor Weteschappelik Onderzoek (NWO)], and by the Foundation for Fundamental Research into Material [Fundamental Onderzoek der Materie (FOM)].

---

*Present address: Natuurkundig Laboratorium, Free University, PB7161, NL-1007 MC Amsterdam, The Netherlands.

†Present address: Solid State Structural Chemistry Unit, Indian Institute of Science, Bangalore 560 012, India.

‡Permanent address: Physical Metallurgy Division, Babha Atomic Research Center, Bombay 400 085, India.

[1]A. R. Williams, C. D. Gelatt, J. W. D. Connolly, and V. L. Moruzzi in *Alloy Phase Diagrams,* edited by L. H. Bennett, J. Massalski, and M. Griesse (North-Holland, Amsterdam, 1982), p. 17.

[2]D. G. Pettifor and R. Podloucky, J. Phys. C **19**, 315 (1986).

[3]C. Calandra, O. Bisi, and G. Ottoviani, Surf. Sci. Rep. **4**, 271 (1985).

[4]O. Bisi and C. Calandra, J. Phys. C **14**, 5479 (1981).

[5]O. Bisi and L. W. Chiao, Phys. Rev. B **25**, 4943 (1982).

[6]A. Franciosi, J. H. Weaver, D. G. O'Neill, F. A. Schmidt, O. Bisi, and C. Calandra, Phys. Rev. B **28**, 7000 (1983).

[7]R. M. Boulet, A. F. Dunsworth, J. J. Jan, and H. L. Skriver, J. Phys. F **10**, 2197 (1980).

[8]O. Nakanishi, A. Yanare, and A. Hasegawa, J. Magn. Magn. Mater. **15-18**, 879 (1980).

[9]Y. J. Chabal, D. R. Hamann, J. E. Rowe, and M. Schlüter, Phys. Rev. B **25**, 7598 (1982).

[10]J. Tersoff and D. R. Hamann, Phys. Rev. B **28**, 1168 (1983).

[11]B. K. Bhattacharyya, D. M. Bylander, and L. Kleinmann, Phys. Rev. B **32**, 7973 (1985).

[12]H. Winter, P. J. Durham, and G. M. Stocks, J. Phys. F **14**, 1047 (1984).

[13]P. Marksteiner, J. Redinger, and P. Weinberger, Z. Phys. B **62**, 443 (1986).

[14]J. H. Weaver, V. L. Moruzzi, and F. A. Schmidt, Phys. Rev. B **23**, 2916 (1981).

[15]A. Franciosi, J. H. Weaver, and F. A. Schmidt, Phys. Rev. B **26**, 546 (1982).

[16]A. Kakizaki, H. Sugawara, I. Nagakura, Y. Ishikawa, T. Komatsubara, and T. Ishii, J. Phys. Soc. Jpn. **51**, 2597, (1982).

[17]J. H. Weaver, A. Franciosi, and V. L. Moruzzi, Phys. Rev. B **29**, 3293 (1984).

[18]J. Beille, D. Bloch, V. Jaccarino, J. H. Wernick, and G. K. Wertheim, J. Phys. (Paris) **38**, 2197 (1975).

[19]M. Azizan, R. Baptist, G. Chauvet, and T. A. Nguyen Tan, Solid State Commun. **57**, 1 (1986).

[20]B. Egert and G. Panzner, Phys. Rev. B **29**, 2091 (1984).

[21]S. J. Oh, J. W. Allen, and J. M. Lawrence, Phys. Rev. B **35**, 2267 (1987).

[22]Ch. Beyreuther and G. Wiech, Phys. Fenn. **9**, 1 (1974).

[23]K. Tanaka, T. Saito, K. Suzuki, and R. Hasegawa, Phys. Rev. B **32**, 6853 (1985).

[24]A. R. Williams, J. Kübler, and C. D. Gelatt, Phys. Rev. B **19**, 6094 (1979).

[25]E. Bucher, S. Schulz, M. Ch. Lux-Steiner, P. Munz, U. Gubler, and G. Greuter, Appl. Phys. A **40**, 71 (1986).

[26]G. K. Wertheim, V. Jaccarino, J. H. Wernick, J. A. Seitchik, H. J. Williams, and R. C. Sherwood, Phys. Lett. **18**, 89 (1965).

[27]W. Speier, J. C. Fuggle, P. Durham, R. Blake, P. Sterne, and R. Zeller, J. Phys. C **21**, 2621 (1988).

[28]L. Ley and M. Cardona, in *Photoemission in Solids II,* edited by L. Ley and M. Cardona (Springer-Verlag, Berlin, 1979), pp. 56ff, and references therein.

[29]J. J. Yeh and F. Lindau, At. Data Nucl. Data Tables **32**, 1 (1985).

[30]O. Bisi, C. Calandra, U. del Pennino, P. Sassaroli, and S. Valeri, Phys. Rev. B **30**, 5696 (1984); C. Calandra, O. Bisi, U. del Pennino, S. Valeri, and U. Xi, Surf. Sci. **168**, 164 (1986).

[31]J. Stöhr, F. R. McFeely, G. Apai, P. S. Wehner, and D. A. Shirley, Phys. Rev. B **14**, 4431 (1976).

[32]A. Franciosi and J. H. Weaver, Surf. Sci. **132**, 324 (1983).

[33]G. W. Rubloff, Surf. Sci. **132**, 268 (1983).

[34]J. C. Fuggle, E. Källne, L. M. Watson, and D. J. Fabian, Phys. Rev. B **16**, 750 (1977).

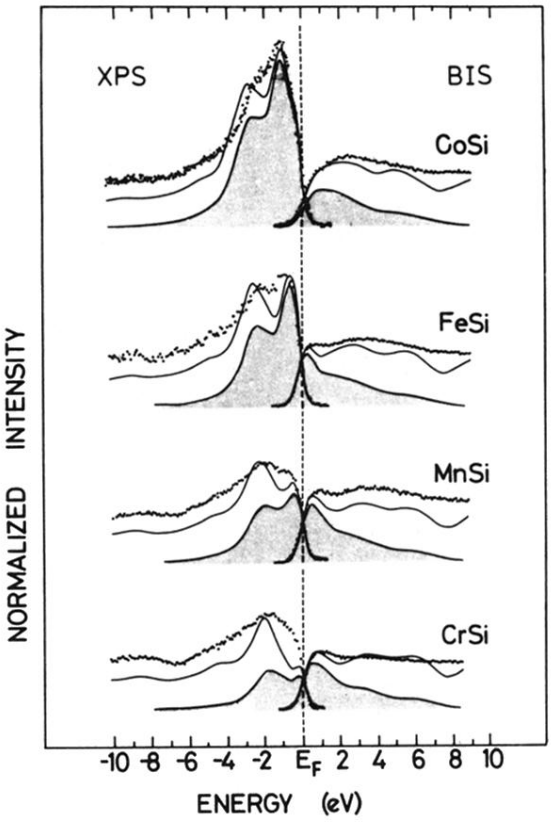

FIG. 5. XPS and BIS spectra for the 3*d* TM monosilicides compared with the theoretical spectra, including matrix elements. Note that here the spectra are normalized with the aid of the theoretical spectrum of CoSi. The metal *d* contribution to the total intensity is shaded.

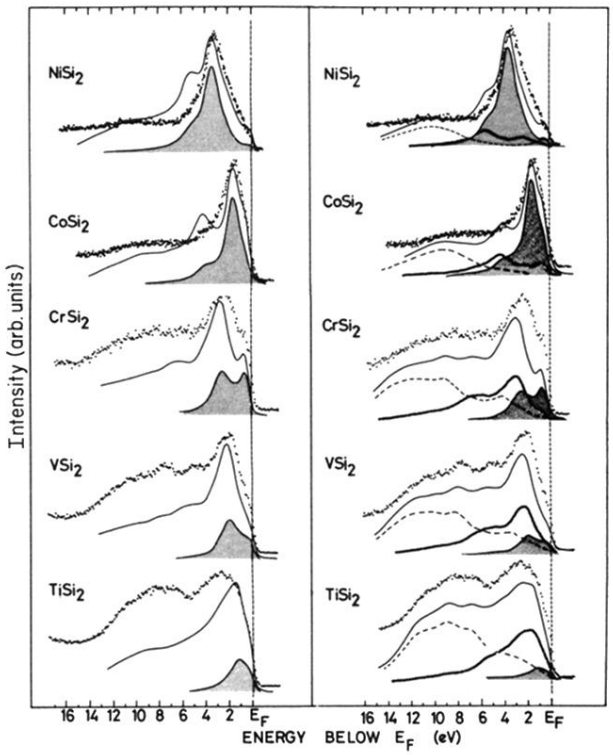

FIG. 6. XPS and BIS spectra for the 3*d* TM disilicides compared with the broadened DOS (left-hand side) and with the theoretical spectra, including matrix elements (right-hand side). Also shown are the calculated partial density of metal *d* states for the left-hand side and the Si (— — —) and *p* (○○○) contributions to the spectra on the right-hand side. The metal *d* contribution is shaded.